NEURAL REGENERATION RESEARCH
www.nrronline.org

Research Article

Modified constraint-induced movement therapy enhances cortical plasticity in a rat model of traumatic brain injury: a resting-state functional MRI study

Cheng-Cheng Sun[1, #], Yu-Wen Zhang[2, #], Xiang-Xin Xing[3, 4, 5, #], Qi Yang[1], Ling-Yun Cao[4], Yu-Feng Cheng[4], Jing-Wang Zhao[4], Shao-Ting Zhou[6], Dan-Dan Cheng[7], Ye Zhang[8], Xu-Yun Hua[3, 9, 10, *], He Wang[2, 11, 12, *], Dong-Sheng Xu[3, 4, 5, *]

https://doi.org/10.4103/1673-5374.344832

Date of submission: November 23, 2021

Date of decision: January 12, 2022

Date of acceptance: April 19, 2022

Date of web publication: June 2, 2022

From the Contents

Graphical Abstract

mCIMT improves motor function of the affected limb after TBI through functional remodeling

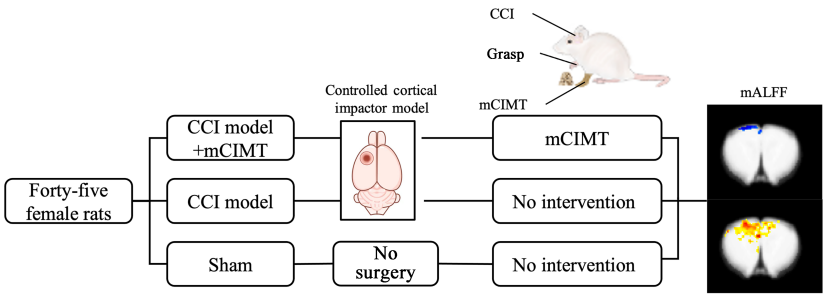

Abstract

Modified constraint-induced movement therapy (mCIMT) has shown beneficial effects on motor function improvement after brain injury, but the exact mechanism remains unclear. In this study, amplitude of low frequency fluctuation (ALFF) metrics measured by resting-state functional magnetic resonance imaging was obtained to investigate the efficacy and mechanism of mCIMT in a control cortical impact (CCI) rat model simulating traumatic brain injury. At 3 days after control cortical impact model establishment, we found that the mean ALFF (mALFF) signals were decreased in the left motor cortex, somatosensory cortex, insula cortex and the right motor cortex, and were increased in the right corpus callosum. After 3 weeks of an 8-hour daily mCIMT treatment, the mALFF values were significantly increased in the bilateral hemispheres compared with those at 3 days postoperatively. The mALFF signal values of left corpus callosum, left somatosensory cortex, right medial prefrontal cortex, right motor cortex, left postero dorsal hippocampus, left motor cortex, right corpus callosum, and right somatosensory cortex were increased in the mCIMT group compared with the control cortical impact group. Finally, we identified brain regions with significantly decreased mALFF values at 3 days postoperatively. Pearson correlation coefficients with the right forelimb sliding score indicated that the improvement in motor function of the affected upper limb was associated with an increase in mALFF values in these brain regions. Our findings suggest that functional cortical plasticity changes after brain injury, and that mCIMT is an effective method to improve affected upper limb motor function by promoting bilateral hemispheric cortical remodeling. mALFF values correlate with behavioral changes and can potentially be used as biomarkers to assess dynamic cortical plasticity after traumatic brain injury.

Key Words: amplitude of low frequency fluctuation; cortical plasticity; functional magnetic resonance imaging; modified constraint-induced movement therapy; traumatic brain injury

Introduction

Traumatic brain injury (TBI), which causes serious damage to the central nervous system, has imposed a heavy burden on individuals, families and society (Jiang et al., 2019; Jamjoom et al., 2021). It not only causes motor dysfunction, but for people with mild or chronic symptoms, there is also a risk of vascular dementia, chronic traumatic encephalopathy, and memory impairment (Mallas et al., 2021). With the progress of basic research and clinical research, the application of regenerative medicine, such as stem cells and exosomes (Zhang et al., 2019), and neuromodulation techniques, including transcranial magnetic stimulation, transcranial electrical stimulation and brain-computer interfaces, in central nervous system diseases have brought exciting advancements; however, some forms of dysfunction remain untreatable, particularly fine motor hand movement (Bao et al., 2020). Multiple studies have shown that exercise therapy, as the final strategy common among all TBI treatments, has a positive impact on patients with brain injury and is an irreplaceable treatment (Stinear et al., 2020).

Compared with other forms of kinesiotherapy, passive exercise, forced exercise and proprioceptive neuromuscular facilitation, modified constraint-induced movement therapy (mCIMT) has a unique clinical application for overcoming upper limb disorders after stroke and is currently the most

[1]Department of Rehabilitation, Tongji Hospital, School of Medicine, Tongji University, Shanghai, China; [2]Institute of Science and Technology for Brain-Inspired Intelligence, Fudan University, Shanghai, China; [3]Center of Rehabilitation Medicine, Yueyang Hospital of Integrated Traditional Chinese and Western Medicine, Shanghai, China; [4]Institute of Rehabilitation Medicine, School of Rehabilitation Science, Shanghai University of Traditional Chinese Medicine, Shanghai, China; [5]Engineering Research Center of Traditional Chinese Medicine Intelligent Rehabilitation, Ministry of Education, Shanghai, China; [6]Department of Rehabilitation, Shanghai East Hospital, School of Medicine, Tongji University, Shanghai, China; [7]Department of Rehabilitation, Tongren Hospital, Shanghai Jiao Tong University School of Medicine, Shanghai, China; [8]Department of Rehabilitation, Shanghai Jiao Tong University Affiliated Sixth People's Hospital, Shanghai, China; [9]Department of Traumatology and Orthopedics, Yueyang Hospital, Shanghai University of Traditional Chinese Medicine, Shanghai, China; [10]Department of Rehabilitation, Yangzhi Rehabilitation Hospital, Tongji University, Shanghai, China; [11]Human Phenome Institute, Fudan University, Shanghai, China; [12]Key Laboratory of Computational Neuroscience and Brain-Inspired Intelligence (Fudan University), Ministry of Education, Shanghai, China

***Correspondence to:** Dong-Sheng Xu, MD, dxu0927@shutcm.edu.cn; He Wang, PhD, hewang@fudan.edu.cn; Xu-Yun Hua, MD, PhD, swrhxy@126.com.
https://orcid.org/0000-0002-8477-5377 (Dong-Sheng Xu); https://orcid.org/0000-0002-2053-9439 (He Wang); https://orcid.org/0000-0002-2935-7551 (Xu-Yun Hua)
#These authors contributed equally to this work.

Funding: *This project was supported by the National Key R&D Program of China, Nos. 2020YFC2004202 (to DSX), 2018YFC2001600 (to XYH); the National Natural Science Foundation of China, Nos. 81974358 (to DSX), 81802249 (to XYH) and 82172554 (to XYH).*

How to cite this article: *Sun CC, Zhang YW, Xing XX, Yang Q, Cao LY, Cheng YF, Zhao JW, Zhou ST, Cheng DD, Zhang Y, Hua XY, Wang H, Xu DS (2023) Modified constraint-induced movement therapy enhances cortical plasticity in a rat model of traumatic brain injury: a resting-state functional MRI study. Neural Regen Res 18(2):410-415.*

studied rehabilitation intervention for patients (Langhorne et al., 2011). It is believed that the therapeutic effects of CIMT involve two main mechanisms: (1) nonuse behavioral mechanisms involved in overcoming learning (Wittenberg and Schaechter, 2009), and (2) neurological mechanisms involved in promoting changes in neuroplasticity (Schaechter et al., 2002; Kononen et al., 2012). A longitudinal follow-up trial demonstrated that mCIMT improved motor function and the effects were maintained for 1 to 2 years (Wolf et al., 2006, 2008). Several clinical and basic studies have found that CIMT improves upper limb motor dysfunction (Barzel et al., 2015; Hu et al., 2021).

Advanced neuroimaging has been used to capture brain morphometry, microstructure, biochemical and metabolic abnormalities after TBI (Smith et al., 2019; Wiegand et al., 2021), including T1/T2-weighted magnetic resonance imaging (MRI) (Smith et al., 2019), diffusion MRI (Dailey et al., 2018), magnetic resonance spectroscopy (Veeramuthu et al., 2018) and positron emission tomography (Graham and Sharp, 2019). To date, the dominant neuroimaging findings in human TBI are changes in volumetric measurements and cortical thickness (Santhanam et al., 2019), white matter microstructure (Rodriguez-Grande et al., 2018), neurochemical concentrations (Lin et al., 2012), and brain metabolism (Ellingson et al., 2019). Furthermore, animal studies have shown that architectural alterations in TBI may be attributed to neuronal and synaptic deficits (Fidan et al., 2018), and diffusion and anomalous metabolism possibly result from neuroinflammation and axonal damage (San Martin Molina et al., 2020). Post-injury neuronal restructuring and plasticity starts in the early stages, lasts for weeks or even years, and involves brain areas far from the affected region. Amplitude of low frequency fluctuation (ALFF) is the square root of the power spectrum between 0.01 and 0.08 Hz in the resting-state functional MRI (rsfMRI) signal. There is an association between ALFF of different brain regions, which is thought to reflect the density of regional spontaneous brain activity. ALFF can be used to indirectly to measure changes in neurons not only temporally, but also spatially.

There are different theories of restoration after brain injury: one is the compensatory theory, and the other is the interhemispheric competition theory, which is the most widely used in clinical practice. The interhemispheric competition theory suggests that once one hemisphere is affected, the balance of interconnection and restraint between the two hemispheres is disrupted and the healthy hemisphere becomes overactivated, which limits the functional recovery of the affected hemisphere (Kerr, 2021). Neuromodulation is a rehabilitation method widely carried out in clinical practice and animal experiments (Hilderley et al., 2019), and it has been confirmed in previous studies that it promotes neuroplasticity (Gao et al., 2020b). Numerous studies of non-invasive brain stimulation based on this theory have demonstrated facilitation of motor recovery, but there are also studies with limited or even opposing results. A critical new model, the bimodal balance–recovery model, was proposed for personalized training (Di Pino et al., 2014). This model links interhemispheric balance and functional recovery to the structural reserve preserved by the lesion. According to this theory, when the injury area is small, compensation of the injured hemisphere is important, and inhibition of the injured hemisphere by the healthy hemisphere is appropriately suppressed. When the injury area is large, then the injured hemisphere depends on the compensation of the healthy hemisphere.

The heterogeneity of human brain injury makes it difficult to obtain good longitudinal follow-up data. At present, it is difficult to collect rsfMRI for patients with brain injury in the early phase, so it is difficult to study changes in patients over time (Van Horn et al., 2017; Jolly et al., 2021). Animal experiments not only allow for imaging acquisition before injury, early post-injury and post-CIMT treatment, but also allow for investigation of the pathophysiological changes after TBI. In our study, in contrast to previous small-sample clinical trials and animal experiments with cerebral ischemia models, we adopted the control cortical impact (CCI) model, which can more precisely simulate the corresponding motor cortex injury of the upper limb. We hypothesized that CIMT can improve functional outcomes in rats with TBI possibly through functional plasticity, by inhibiting the motor cortex of the unaffected hemisphere to reduce the abnormal inhibition of the affected hemisphere, or to stimulate the motor cortex of the affected hemisphere, leading to improved behavioral performance in rats.

Methods

Animals

Forty-five specific pathogen free Sprague-Dawley rats (female, weighing 250 to 300 g, 8–10 weeks old) were provided by SLAC Laboratory Animal Co., Ltd. in Shanghai, China (license number: SCXK (Hu) 2017-0005). All animals were housed with three to four rats per cage at a regulated temperature (23°C) with a 12-hour light/dark cycle and *ad libitum* access to water. Rats were randomly allocated using the random number table method to either the sham group (Sham; n = 15), CCI group (CCI; n = 15), or mCIMT group (mCIMT; n = 15). The study protocol met animal ethical standards and was granted approval by the Animal Ethics Committee of Tongji University Hospital, China on October 13, 2020 (approval No. 2020-DW-002). This study was reported in accordance with the Animal Research: Reporting of *In Vivo* Experiments 2.0 guidelines (Percie du Sert et al., 2020).

CCI model

The CCI model was established as previously described (Shultz et al., 2017). Anesthesia was induced by 4% isoflurane (RWD Life Science Co., Ltd, Shenzhen, China) inhalation and maintained with 2.5% isoflurane via a mask placed over the mouth. Rectal temperature was measured and maintained at 36.5–37.5°C with a heating pad. The animal was placed in a rat stereotaxic apparatus fixed with ear and incisor bars (RWD Life Science Co., Ltd, Shenzhen, China). A 5.0-mm circular craniectomy was performed using a drill in the left parietal cortex (from the bregma: 0.5 to 4.5 mm anterior-posterior, 0 to 5 mm medial-lateral) according to the Rat Brain in Stereotaxic Coordinates (Paxinos and Watson, 1998) without any damage. After the craniectomy, the CCI device with a 5.0-mm planar impactor tip (YHCI99, Wuhan Yihong Technology Co., Ltd., Wuhan, Hubei Province, China) was placed in the center of the craniectomy site. Moderate injury was induced at a speed of 4 m/s, a dwell time of 150 ms, and a deformation depth of 2.8 mm. The sham group received the same procedure except for the impact. The animal was placed in a heated chamber until the effect of anesthesia wore off and was then returned to its cage. Rats were acclimated to the environment and pretrained (i.e. grasped) for 2 weeks. Preoperative and postoperative (3 and 28 days) cylinder rearing tests and MRI acquisitions were performed. One week after CCI, rats in the mCIMT group were treated with mCIMT (**Figure 1**).

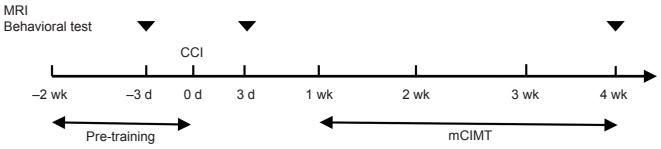

Figure 1 | **Experimental design.**
CCI: Control cortical impact; mCIMT: modified constraint-induced movement therapy.

mCIMT

The mCIMT training started 1 week after surgery and was usually performed at the same time each day. Rats were stabilized with a moderate elastic plaster, lined with cotton to prevent direct contact with the skin, on the healthy side forelimb (left) for 8 hours per day for 3 weeks. The injured side forelimb (right) was forced to grasp food for training for 1 hour. The rat was placed in a 30 cm × 35 cm rectangular box made of acrylic plates, with a small window 15 cm high and 1 cm wide on the side of the box and a small shelf outside the window. Peanut rice cut into small pellets was placed on the shelf. A successful test was one in which the rat grasped, fetched and took the small pellet to its mouth. A failed test was one in which the pellet was not captured, failed to be captured, or dropped. After training, the rats were given enough food for one day to continue grasping food with the affected hand, and no food was given outside of training/restraint. Rats in the other groups moved freely in the cage without any restraint.

Cylinder rearing test

The cylinder rearing test (Emerick and Kartje, 2004) was used to assess forelimb asymmetry at baseline, and at 3 days and 28 days after CCI. The rat was placed in a glass resin cylinder (25 cm × 30 cm) with two mirrors on either side, and was allowed to rear and place their forepaws on the cylinder wall for 5 minutes. A video camera recorded the rat standing and moving, and analyzed the number of times the forelimb walls made contact and slid. The sliding score of the right forelimb was determined using the following formula: (right forelimb sliding times/right forelimb total touches) × 100%.

MRI acquisition

Brain fMRI scans were conducted on the three groups of rats with a Bruker 11.7 T MRI system (Bruker Medizintechnik, Karlsruhe, Germany) at baseline, and at 3 and 28 days after CCI surgery. After anesthesia was induced by 4% isoflurane, the rat was fastened to the scanner and its body temperature was maintained at 37.5°C by a heating pad with a water bath. Continuous anesthesia was maintained with 1–2.5% isoflurane with ventilator support and respiratory monitoring. For the imaging, an interleaved single EPI sequence was used with the following parameters: flip angle, 90°; slice thickness, 0.3 mm; repetition time, 3000 ms; echo time, 8.538 ms; mean value, 1; field of view, 27 × 27 mm^2 with 90 × 90.

MRI data preprocessing

Data preprocessing was carried out using the Statistical Parametric Mapping 12 (SPM 12) toolbox (http://www.fil.ion.ucl.ac.uk/spm/), which is based on the MATLAB 2013b platform (MathWorks, Natick, MA, USA). Rats with head movement greater than 0.2 mm or head rotation greater than 0.2° in either direction were excluded. Firstly, the first 10 time points were removed and the images were augmented by up to 10 × 10 × 10 times to match the size of the human brain without the need for interpolation, which allowed for developing processing algorithms that were initially designed for human data. Secondly, non-brain tissue was manually removed before further preprocessing. Slice timing procedures were used to correct the fMRI images to remove timing bias from the slice acquisition. A rigid body transformation was used to spatially realign the images to correct for voxel misalignment that was caused by head motion. Normalization of the standard space was realized using a standard brain template with a voxel size of 2.06 × 2.06 × 2 for the normalized images (Schwarz et al., 2006). Images were subsequently smoothed by full-width half-maximum quadruplication to voxel size 4.12 × 4.12 × 4. Additional preprocessing included regression, detrending and filtering (0.01–0.08 Hz) of interfering signals to reduce the effects of low frequency linear drift and high frequency physiological breathing and noise.

Mean ALFF analyses

Following data preprocessing, REST (Beijing Normal University, http://www.restfmri.net) was used to calculate the ALFF data (Song et al., 2011). The time series of each voxel was converted to the frequency domain using the fast Fourier transform. The power spectrum in the frequency band of each voxel was obtained. Given that the power at a given frequency is proportional to the square of the amplitude of that frequency component, the square root of the power spectrum was obtained for each frequency. Then the average square root (ALFF value) of the power at different frequency bands was calculated (Yang et al., 2007). Finally, the ALFF values for each animal were converted to mean ALFF (mALFF) by dividing the ALFF of each voxel by the global average ALFF for further comparisons between groups.

Statistical analysis

No statistical methods were used to predetermine the sample sizes; however, our sample sizes were similar to those reported in a previous publication (Zheng et al., 2020). Behavioral analyses were performed blind to whether CCI modeling and mCIMT treatment were performed, whereas MRI examinations and analyses were not performed blind to experimental conditions. To longitudinally observe the mALFF differences between the three groups, we performed a two-sample *t*-test in SPM12 software implemented in MATLAB 2013b (MathWorks, Sherborn, MA, USA) for individual mALFF maps at different times for each pair of the three groups with a mask, which corresponds to a corrected $P < 0.005$. To investigate the relationship between the mALFF and upper limb motor function performance, we selected brain regions with significant changes in mALFF values at 3 days after injury as a mask. The mALFF signal values were extracted from the three groups at 3 and 28 days postoperatively. Pearson correlation coefficients between mALFF values and right forelimb glide scores were calculated using GraphPad Prism 7 (GraphPad, San Diego, CA, USA, www.graphpad.com) and the threshold for significance was set at $P < 0.05$.

Results

CCI group and sham group differences in mALFF maps on day 3 after surgery

Figure 2 shows a two sample *t*-test analysis between the CCI group and Sham group mALFF maps. After CCI surgery, the most significant mALFF decrease in the CCI group was found in the left motor cortex, and decreases were also seen in the left somatosensory cortex, left cortex insular, and right motor cortex. An increase in mALFF in the CCI group was observed in the right corpus callosum. See **Table 1** for a list of these regions.

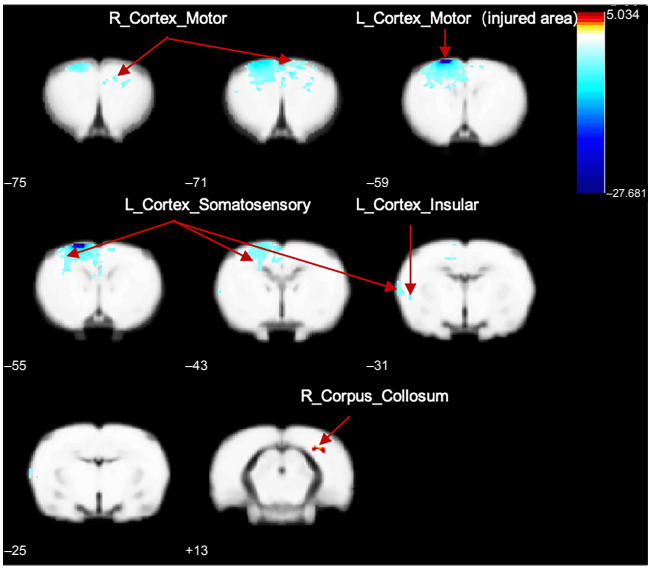

Figure 2 | mALFF maps in rats between the CCI group and sham group 3 days after surgery.
The warm tone represents areas where the mALFF values of the CCI group were higher than those of the sham group, and the cold tone represents areas where mALFF values of the CCI group were lower than those of the sham group. The numbers in the graph represent the Z-axis coordinates along the anterior-posterior axis, referencing the stereotaxic rat brain magnetic resonance imaging template, with which the coordinates of Paxinos and Watson (1998) have been aligned. The statistical threshold was set at $P < 0.005$. Notably, we show the results of a two-sample *t*-test in the mask showing the sensorimotor correlation network. CCI: Control cortical impact; mALFF: mean amplitude of low frequency fluctuation.

mALFF maps of the mCIMT group between day 3 and day 28 after surgery

Figure 3 shows a two sample *t*-test analysis of the mCIMT group mALFF maps between the 3rd day and 28th day after surgery. On day 28, the mALFF signals of the left motor cortex, left medial prefrontal cortex, left postero dorsal hippocampus, left corpus callosum, right motor cortex, right somatosensory cortex, right corpus callosum, and left frontal association cortex were significantly increased compared with those on day 3. See **Table 2** for a list of these regions.

Table 1 | Brain regions showing mALFF differences between the CCI and sham groups 3 days after surgery

	Brain regions	No. of voxels	Peak *t*-value	MNI coordinates (mm)		
				x	*y*	*z*
CCI > Sham	R_Corpus_Collosum	25	5.034	44	17	13
CCI < Sham	L_Cortex_Motor	4086	−27.681	−17	40	−55
	L_Cortex_Somatosensory	294	−3.396	−34	28	−59
	L_Cortex_Insular	294	−4.848	−57	−18	−31
	R_Cortex_Motor	87	−4.156	18	34	−57

A two-sample *t*-test was used to identify significant voxels. The *P* value was set to 0.005 and the corresponding *t*-value was then determined by the *P* value. *x*, *y*, *z*: coordinates of the position of the primary peak in MNI space. CCI: Control cortical impact; L: left; MNI: Montreal Neurological Institute; R: right.

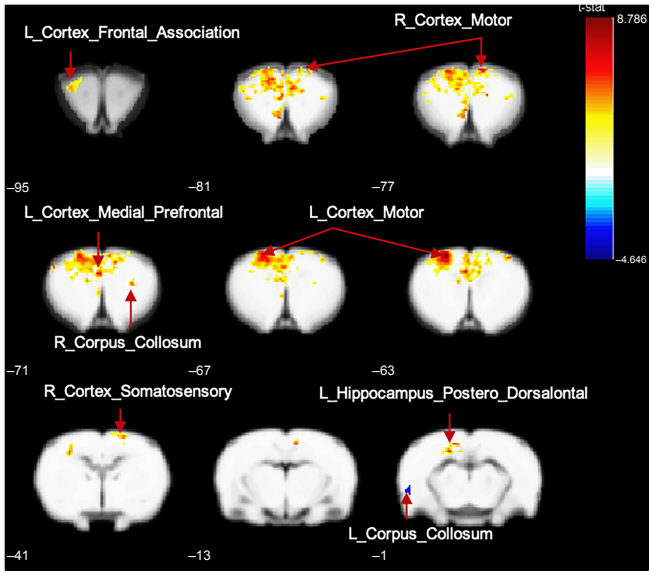

Figure 3 | mALFF maps of the mCIMT group between 3 days and 28 days after surgery.
The warm tone represents areas where mALFF values at 28 days were higher than those at 3 days, and the cold tone represents areas where mALFF values at 28 days were lower than those at 3 days. The numbers in the figure are the coordinates of the *Z*-axis in standard space. The statistical threshold was set at $P < 0.005$. Of note, we showed the two-sample *t*-tests results within a mask showing sensorimotor-related networks. CCI: Control cortical impact; mALFF: mean amplitude of low frequency fluctuation.

Table 2 | Brain regions showing mALFF differences of mCIMT group between 3 days and 28 days after surgery

	Brain regions	No. of voxels	Peak *t*-value	MNI coordinates (mm)		
				x	*y*	*z*
28 d > 3 d	L_Cortex_Motor	4063	8.786	−23	34	−63
	L_Cortex_Medial_Prefrontal	4063	7.114	−3	15	−71
	L_Hippocampus_Postero_Dorsal	241	5.195	−19	22	−1
	L_Corpus_Collosum	241	4.024	−36	13	19
	R_Cortex_Motor	56	4.91	12	30	−13
	R_Cortex_Somatosensory	86	4.581	24	38	−41
	R_Corpus_Collosum	21	4.434	32	5	−71
	L_Cortex_Frontal_Association	64	4.174	−34	16	−95
28 d < 3 d	L_Corpus_Collosum	40	−4.646	−63	−24	−1

A two-sample *t*-test was used to identify significant voxels. The *P* value was set to 0.005 and the corresponding *t*-value was then determined by the *P* value. *x*, *y*, *z*: coordinates of the position of the primary peak in MNI space. L: Left; mALFF: mean amplitude of low frequency fluctuation; mCIMT: modified constraint-induced movement therapy; MNI: Montreal Neurological Institute; R: right.

mALFF maps between the mCIMT group and CCI group on day 28 after surgery

Figure 4 shows a two sample *t*-test analysis between the mCIMT group and CCI group mALFF maps 28 days after surgery. Compared with the mALFF values of the CCI group, the mALFF values of the mCIMT group were increased in the left corpus callosum, left somatosensory cortex, right cortex

medial prefrontal, right motor cortex, left postero dorsal hippocampus, left motor cortex, right corpus callosum, and right somatosensory cortex. Conversely, mALFF values in the left somatosensory cortex, right antero dorsal hippocampus, right somatosensory cortex, and right corpus callosum were decreased in the mCIMT group compared with the CCI group. See **Table 3** for a list of these regions.

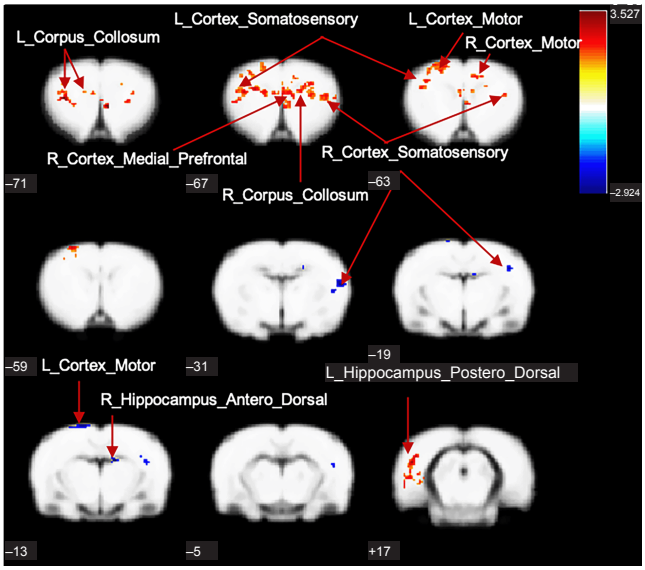

Figure 4 | **mALFF maps between the mCIMT group and CCI group 28 days after surgery.**
The warm tone represents areas where mALFF values of the mCIMT group were higher than those of the CCI group, and the cold tone represents areas where mALFF values of the mCIMT group were lower than those of the CCI group. The numbers in the figure are the coordinates of the *Z*-axis in standard space. The statistical threshold was set at $P < 0.05$. Of note, we showed the two-sample *t*-tests results within a mask showing sensorimotor-related networks. CCI: Control cortical impact; mALFF: mean amplitude of low frequency fluctuation; mCIMT: modified constraint-induced movement therapy.

Table 3 | **Brain regions showing mALFF differences between the CCI group and mCIMT group 28 days after surgery**

	Brain regions	No. of voxels	Peak *t*-value	MNI coordinates (mm)		
				x	*y*	*z*
mCIMT > CCI	L_Corpus_Collosum	454	3.527	–38	1	–71
	L_Cortex_Somatosensory	286	2.424	–40	20	–63
	R_Cortex_Medial_ Prefrontal	219	3.515	9	–7	–71
	R_Cortex_Motor	219	2.799	16	22	–65
	L_Hippocampus_Postero_ Dorsal	111	3.246	–54	5	17
	L_Cortex_Motor	167	2.882	–30	38	–59
	R_Corpus_Collosum	104	2.514	24	13	–67
	R_Cortex_Somatosensory	55	2.339	44	3	–65
mCIMT < CCI	L_Cortex_Somatosensory	57	–2.924	–21	44	–11
	R_Hippocampus_Antero_ Dorsal	106	–2.901	18	7	–13
	R_Cortex_Somatosensory	162	–2.766	63	–1	–31
	R_Corpus_Collosum	70	–2.065	57	1	–5

A two-sample *t*-test was used to identify significant voxels. The *P* value was set to 0.05 and the corresponding *t*-value was then determined by the *P* value. *x*, *y*, *z*: coordinates of the position of the primary peak in MNI space. CCI: Control cortical impact; L: left; mALFF: mean amplitude of low frequency fluctuation; mCIMT: modified constraint-induced movement therapy; MNI: Montreal Neurological Institute; R: right.

Negative correlation between mALFF values and sliding score of the right forelimb

Figure 5 shows the correlation between mALFF values and sliding scores of the right forelimb in all three groups. We selected the negative activation area of the difference between the CCI group and the Sham group in the mALFF map on day 3 as a mask, and extracted mALFF signals of the three groups on days 3 and 28. The mALFF value of this cluster was negatively correlated with the motor performance of the right upper limb ($r = -0.725$, $P < 0.0001$). On day 28, the means ± standard deviation for the sham, CCI, and mCIMT groups were 0.075 ± 0.039, 0.178 ± 0.062, and 0.044 ± 0.155, respectively, which suggested improved behavior in the mCIMT group compared with the CCI group.

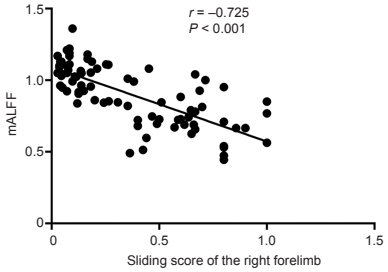

Figure 5 | **Pearson correlation between the mALFF values and sliding score of the right forelimb.**
The analysis indicated a negative correlation between the mALFF and right upper limb motor function performance ($r = -0.725$, $P < 0.001$). The black dots represent the sliding score of the right forelimb for all rats in all three groups at the two time points of 3 and 28 days postoperatively. mALFF: Mean amplitude of low frequency fluctuation.

Discussion

mCIMT has shown beneficial effects in improving motor control and function of the upper limb after TBI, but the exact mechanism remains unclear (Abdullahi et al., 2020). The current consensus is that improved function is associated with changes in synaptic plasticity and cortical recombination. Our study has confirmed that after CCI surgery, in addition to the decrease in the mALFF signal value in the motor cortex of the affected hemisphere, the motor cortex of the contralateral hemisphere also showed a transient signal decrease. This may be due to a decreased connection between the left and right hemispheres by the corpus callosum (Vahdat et al., 2021). In the mCIMT group, mALFF signals of the left motor cortex, left medial prefrontal cortex, left postero dorsal hippocampus, left corpus callosum, right motor cortex, right somatosensory cortex, right corpus callosum, and left frontal association cortex were significantly increased on day 28 compared with those on day 3. We consider that this increase may be related to spontaneous recovery (Thengone et al., 2016) after injury or the efficacy of mCIMT intervention, and that the activated area in the right hemisphere may be a compensatory effect of the healthy hemisphere. To distinguish between spontaneous recovery and mCIMT treatment, the mCIMT group was compared with the CCI group on day 28; the mALFF signal values of left corpus callosum, left somatosensory cortex, right cortex medial prefrontal, right motor cortex, left postero dorsal hippocampus, left motor cortex, right corpus callosum, and right somatosensory cortex were increased in the mCIMT group. These results suggest that mCIMT may improve motor function by activating neuronal plasticity in both the affected hemisphere and the healthy hemisphere. However, this evidence is not convincing enough because the *P*-value was set at 0.05. Nevertheless, this finding is still informative for understanding recovery. Because the CCI model used in this study is moderately severe, its plasticity is limited. mCIMT can promote recovery of motor function through cortical plasticity, but for severe structural damage, based on the bimodal balance–recovery model, it seems to be consistent with the observed mALFF results. Future studies with a range of injury severity should be performed to verify the conclusions.

Although CIMT has been shown to promote motor function recovery after stroke or trauma in clinical and animal research, its repair mechanisms are still being explored (Cimolin et al., 2012; Kwakkel et al., 2015; Nesin et al., 2019). A study in five participants with developmental disregard suggested that contralateral cortical activity was important for improvement of the affected hand movement (Sutcliffe et al., 2009). A study of ALFF in 20 patients with chronic and diffuse trauma reported that increased frontal functional activity at rest was associated with better overall cognitive performance (Palacios et al., 2013). The integrity of the corticospinal tract has been shown to correlate with functional improvement after injury (Rocca et al., 2013b). A single-photon emission computerized tomography study reported that CIMT increased the perfusion of motor areas in patients with chronic stroke (Könönen et al., 2005). Diffusion tensor imaging and rsfMRI offer promising and objective markers to predict clinical outcomes following CIMT in congenital children (Rocca et al., 2013a). A series of research studies suggested that these positive effects occur via the upregulation of postsynaptic membrane α-amino-3-hydroxy-5-methyl-4-isoxazole-propionic acid receptor expression (Hu et al., 2021). They also reported that mCIMT alters synaptic plasticity of the contralateral hippocampus in a middle cerebral artery occlusion rat model (Gao et al., 2020a). In another study, mCIMT not only promoted angiogenesis and neurogenesis after cerebral ischemia/reperfusion, but also promoted the expression of neurotrophic factors (Zhao et al., 2013). In contrast, an experimental stroke study reported that granulocyte-colony stimulating factor enhanced recovery, whereas CIMT had no effect on recovery (Diederich et al., 2012). The varied findings could be explained by a number of reasons, including limited sample sizes, different injury levels of the models, and timing of intervention. In addition, these studies did not systematically study the time-dependent dynamic remodeling of cortical sensorimotor networks.

The innovation of this study is that we not only evaluated the effects of CIMT on motor function after TBI through mALFF signals, but we also observed

the longitudinal changes before and after the injury and treatment. The CCI animal model allows for accurate control of the impact location, which is more conducive to exploring repair mechanisms. In addition, further molecular biological and pathological tissue staining should be performed to verify the rsfMRI results. Finally, using the current theoretical guidance and results, future studies should conduct neuromodulation in rats to provide a clinical paradigm for the combination of mCIMT and neuromodulation (Grefkes and Fink, 2011; Hartwigsen and Volz, 2021).

Our study has some limitations. We focused only on the mALFF, but not on the functional connectivity between different brain regions and the changes between different brain networks. In future studies, we will analyze the functional connections between brain regions, and the connections between brain networks, and combine this with neural regulation to investigate the regulation of functional connectivity and its role in motor function recovery. Additionally, neuroinflammation is an important driver of secondary injury after TBI, but we did not assess neuroinflammatory factors. We will analyze these in future experiments.

There are some common issues of rehabilitation interventions that we need to consider. First, there is no scale gradient from mild to severe brain injury in injury models. In ischemic models with small area injury, where the theory of interhemispheric competition dominates, early mCIMT may be beneficial. However, for moderate to severe injury, according to the bimodal balance-recovery model, the compensatory effect of the healthy brain hemisphere may have a bigger effect than suppressing its excitability. Second, in terms of the timing of intervention, premature forced movement of the affected upper limbs may lead to faulty compensation patterns rather than recovery (Jones, 2017), which is detrimental to motor function recovery. mCIMT interventions that are too late may miss the optimal timing for rehabilitation. Therefore, in future experiments, the injury area and the timing of intervention should be taken into account.

Conclusions

These preliminary findings suggest that after brain injury, brain function changed dynamically, and motor function improvements produced by mCIMT were accompanied by brain plasticity reorganization, which may promote recovery. mALFF can be used as a sensitive indicator to assess dynamic changes in brain plasticity and thus provides guidance for further treatment. Further histological and multimodal neuroimaging studies are needed to confirm these results. Nevertheless, animal studies and neuroimaging in TBI may lead to the identification of target biomarkers and the development of more targeted clinical neuromodulation techniques.

Author contributions: *Study design: CCS, XYH, DSX; experimental implementation: CCS, YWZ, QY, YZ, YFC; MRI data analysis: XXX, LYC, JWZ, STZ; manuscript writing: CCS, DDC; experiment supervision: HW, DSX, statistical analysis supervision: XYH, and manuscript revising: XYH, DSX, HW. All authors read and approved the final manuscript.*
Conflicts of interest: *The authors declare no conflict of interest.*
Availability of data and materials: *All data generated or analyzed during this study are included in this published article and its supplementary information files.*

Open peer reviewers: *Jianmin Zhang, The Second Affiliated Hospital of Zhejiang University School of Medicine, USA; Emily Petrus, National Institutes of Health, USA.*
Additional file: *Open peer review reports 1 and 2.*

References

Abdullahi A, Truijen S, Saeys W (2020) Neurobiology of recovery of motor function after stroke: the central nervous system biomarker effects of constraint-induced movement therapy. Neural Plast 2020:9484298.

Bao SC, Khan A, Song R, Kai-Yu Tong R (2020) Rewiring the lesioned brain: electrical stimulation for post-stroke motor restoration. J Stroke 22:47-63.

Barzel A, Ketels G, Stark A, Tetzlaff B, Daubmann A, Wegscheider K, van den Bussche H, Scherer M (2015) Home-based constraint-induced movement therapy for patients with upper limb dysfunction after stroke (HOMECIMT): a cluster-randomised, controlled trial. Lancet Neurol 14:893-902.

Cimolin V, Beretta E, Piccinini L, Turconi AC, Locatelli F, Galli M, Strazzer S (2012) Constraint-induced movement therapy for children with hemiplegia after traumatic brain injury: a quantitative study. J Head Trauma Rehabil 27:177-187.

Dailey NS, Smith R, Bajaj S, Alkozei A, Gottschlich MK, Raikes AC, Satterfield BC, Killgore WDS (2018) Elevated aggression and reduced white matter integrity in mild traumatic brain injury: a DTI study. Front Behav Neurosci 12:118.

Di Pino G, Pellegrino G, Assenza G, Capone F, Ferreri F, Formica D, Ranieri F, Tombini M, Ziemann U, Rothwell JC, Di Lazzaro V (2014) Modulation of brain plasticity in stroke: a novel model for neurorehabilitation. Nat Rev Neurol 10:597-608.

Diederich K, Quennet V, Bauer H, Muller HD, Wersching H, Schabitz WR, Minnerup J, Sommer C (2012) Successful regeneration after experimental stroke by granulocyte-colony stimulating factor is not further enhanced by constraint-induced movement therapy either in concurrent or in sequential combination therapy. Stroke 43:185-192.

Ellingson BM, Yao J, Raymond C, Chakhoyan A, Khatibi K, Salamon N, Villablanca JP, Wanner I, Real CR, Laiwalla A, McArthur DL, Monti MM, Hovda DA, Vespa PM (2019) pH-weighted molecular MRI in human traumatic brain injury (TBI) using amine proton chemical exchange saturation transfer echoplanar imaging (CEST EPI). Neuroimage Clin 22:101736.

Emerick AJ, Kartje GL (2004) Behavioral recovery and anatomical plasticity in adult rats after cortical lesion and treatment with monoclonal antibody IN-1. Behav Brain Res 152:315-325.

Fidan E, Foley LM, New LA, Alexander H, Kochanek PM, Hitchens TK, Bayir H (2018) Metabolic and structural imaging at 7 tesla after repetitive mild traumatic brain injury in immature rats. ASN Neuro 10:1759091418770543.

Gao BY, Xu DS, Liu PL, Li C, Du L, Hua Y, Hu J, Hou JY, Bai YL (2020a) Modified constraint-induced movement therapy alters synaptic plasticity of rat contralateral hippocampus following middle cerebral artery occlusion. Neural Regen Res 15:1045-1057.

Gao BY, Sun CC, Xia GH, Zhou ST, Zhang Y, Mao YR, Liu PL, Zheng Y, Zhao D, Li XT, Xu J, Xu DS, Bai YL (2020b) Paired associated magnetic stimulation promotes neural repair in the rat middle cerebral artery occlusion model of stroke. Neural Regen Res 15:2047-2056.

Graham NS, Sharp DJ (2019) Understanding neurodegeneration after traumatic brain injury: from mechanisms to clinical trials in dementia. J Neurol Neurosurg Psychiatry 90:1221-1233.

Grefkes C, Fink GR (2011) Reorganization of cerebral networks after stroke: new insights from neuroimaging with connectivity approaches. Brain 134:1264-1276.

Hartwigsen G, Volz LJ (2021) Probing rapid network reorganization of motor and language functions via neuromodulation and neuroimaging. Neuroimage 224:117449.

Hilderley AJ, Metzler MJ, Kirton A (2019) Noninvasive neuromodulation to promote motor skill gains after perinatal stroke. Stroke 50:233-239.

Hu J, Liu PL, Hua Y, Gao BY, Wang YY, Bai YL, Chen C (2021) Constraint-induced movement therapy enhances AMPA receptor-dependent synaptic plasticity in the ipsilateral hemisphere following ischemic stroke. Neural Regen Res 16:319-324.

Jamjoom AAB, Rhodes J, Andrews PJD, Grant SGN (2021) The synapse in traumatic brain injury. Brain 144:18-31.

Jiang JY, Gao GY, Feng JF, Mao Q, Chen LG, Yang XF, Liu JF, Wang YH, Qiu BH, Huang XJ (2019) Traumatic brain injury in China. Lancet Neurol 18:286-295.

Jolly AE, Balaet M, Azor A, Friedland D, Sandrone S, Graham NSN, Zimmerman K, Sharp DJ (2021) Detecting axonal injury in individual patients after traumatic brain injury. Brain 144:92-113.

Jones TA (2017) Motor compensation and its effects on neural reorganization after stroke. Nat Rev Neurosci 18:267-280.

Kerr AL (2021) Contralesional plasticity following constraint-induced movement therapy benefits outcome: contributions of the intact hemisphere to functional recovery. Rev Neurosci doi: 10.1515/revneuro-2021-0085.

Kononen M, Tarkka IM, Niskanen E, Pihlajamaki M, Mervaala E, Pitkanen K, Vanninen R (2012) Functional MRI and motor behavioral changes obtained with constraint-induced movement therapy in chronic stroke. Eur J Neurol 19:578-586.

Könönen M, Kuikka JT, Husso-Saastamoinen M, Vanninen E, Vanninen R, Soimakallio S, Mervaala E, Sivenius J, Pitkänen K, Tarkka IM (2005) Increased perfusion in motor areas after constraint-induced movement therapy in chronic stroke: a single-photon emission computerized tomography study. J Cereb Blood Flow Metab 25:1668-1674.

Kwakkel G, Veerbeek JM, van Wegen EE, Wolf SL (2015) Constraint-induced movement therapy after stroke. Lancet Neurol 14:224-234.

Langhorne P, Bernhardt J, Kwakkel G (2011) Stroke rehabilitation. Lancet 377:1693-1702.

Lin AP, Liao HJ, Merugumala SK, Prabhu SP, Meehan WP, 3rd, Ross BD (2012) Metabolic imaging of mild traumatic brain injury. Brain Imaging Behav 6:208-223.

Mallas EJ, De Simoni S, Scott G, Jolly AE, Hampshire A, Li LM, Bourke NJ, Roberts SAG, Gorgoraptis N, Sharp DJ (2021) Abnormal dorsal attention network activation in memory impairment after traumatic brain injury. Brain 144:114-127.

Nesin SM, Sabitha KR, Gupta A, Laxmi TR (2019) Constraint induced movement therapy as a rehabilitative strategy for ischemic stroke-linking neural plasticity with restoration of skilled movements. J Stroke Cerebrovasc Dis 28:1640-1653.

Palacios EM, Sala-Llonch R, Junque C, Roig T, Tormos JM, Bargallo N, Vendrell P (2013) Resting-state functional magnetic resonance imaging activity and connectivity and cognitive outcome in traumatic brain injury. JAMA Neurol 70:845-851.

Paxinos G, Watson C (1998) The rat brain in stereotaxic coordinates, 4th ed. San Diego: Academic Press.

Percie du Sert N, Hurst V, Ahluwalia A, Alam S, Avey MT, Baker M, Browne WJ, Clark A, Cuthill IC, Dirnagl U, Emerson M, Garner P, Holgate ST, Howells DW, Karp NA, Lazic SE, Lidster K, MacCallum CJ, Macleod M, Pearl EJ, et al. (2020) The ARRIVE guidelines 2.0: Updated guidelines for reporting animal research. PLoS Biol 18:e3000410.

Rocca MA, Turconi AC, Strazzer S, Absinta M, Valsasina P, Beretta E, Copetti M, Cazzagon M, Falini A, Filippi M (2013) MRI predicts efficacy of constraint-induced movement therapy in children with brain injury. Neurotherapeutics 10:511-519.

Rocca MA, Turconi AC, Strazzer S, Absinta M, Valsasina P, Beretta E, Copetti M, Cazzagon M, Falini A, Filippi M (2013b) MRI predicts efficacy of constraint-induced movement therapy in children with brain injury. Neurotherapeutics 10:511-519.

Rodriguez-Grande B, Obenaus A, Ichkova A, Aussudre J, Bessy T, Barse E, Hiba B, Catheline G, Barriere G, Badaut J (2018) Gliovascular changes precede white matter damage and long-term disorders in juvenile mild closed head injury. Glia 66:1663-1677.

San Martin Molina I, Salo RA, Abdollahzadeh A, Tohka J, Grohn O, Sierra A (2020) In vivo diffusion tensor imaging in acute and subacute phases of mild traumatic brain injury in rats. eNeuro 7:ENEURO.0476-19.2020.

Santhanam P, Wilson SH, Oakes TR, Weaver LK (2019) Accelerated age-related cortical thinning in mild traumatic brain injury. Brain Behav 9:e01161.

Schaechter JD, Kraft E, Hilliard TS, Dijkhuizen RM, Benner T, Finklestein SP, Rosen BR, Cramer SC (2002) Motor recovery and cortical reorganization after constraint-induced movement therapy in stroke patients: a preliminary study. Neurorehabil Neural Repair 16:326-338.

Schwarz AJ, Danckaert A, Reese T, Gozzi A, Paxinos G, Watson C, Merlo-Pich EV, Bifone A (2006) A stereotaxic MRI template set for the rat brain with tissue class distribution maps and co-registered anatomical atlas: application to pharmacological MRI. Neuroimage 32:538-550.

Shultz SR, McDonald SJ, Vonder Haar C, Meconi A, Vink R, van Donkelaar P, Taneja C, Iverson GL, Christie BR (2017) The potential for animal models to provide insight into mild traumatic brain injury: Translational challenges and strategies. Neurosci Biobehav Rev 76(Pt B):396-414.

Smith LGF, Milliron E, Ho ML, Hu HH, Rusin J, Leonard J, Sribnick EA (2019) Advanced neuroimaging in traumatic brain injury: an overview. Neurosurg Focus 47:E17.

Song XW, Dong ZY, Long XY, Li SF, Zuo XN, Zhu CZ, He Y, Yan CG, Zang YF (2011) REST: a toolkit for resting-state functional magnetic resonance imaging data processing. PLoS One 6:e25031.

Stinear CM, Lang CE, Zeiler S, Byblow WD (2020) Advances and challenges in stroke rehabilitation. Lancet Neurol 19:348-360.

Sutcliffe TL, Logan WJ, Fehlings DL (2009) Pediatric constraint-induced movement therapy is associated with increased contralateral cortical activity on functional magnetic resonance imaging. J Child Neurol 24:1230-1235.

Thengone DJ, Voss HU, Fridman EA, Schiff ND (2016) Local changes in network structure contribute to late communication recovery after severe brain injury. Sci Transl Med 8:368re365.

Vahdat S, Pendharkar AV, Chiang T, Harvey S, Uchino H, Cao Z, Kim A, Choy M, Chen H, Lee HJ, Cheng MY, Lee JH, Steinberg GK (2021) Brain-wide neural dynamics of poststroke recovery induced by optogenetic stimulation. Sci Adv 7:eabd9465.

Van Horn JD, Bhattrai A, Irimia A (2017) Multimodal imaging of neurometabolic pathology due to traumatic brain injury. Trends Neurosci 40:39-59.

Veeramuthu V, Seow P, Narayanan V, Wong JHD, Tan LK, Hernowo AT, Ramli N (2018) Neurometabolites alteration in the acute phase of mild traumatic brain injury (mTBI): an in vivo proton magnetic resonance spectroscopy (1H-MRS) study. Acad Radiol 25:1167-1177.

Wiegand TLT, Sollmann N, Bonke EM, Umeasalugo KE, Sobolewski KR, Plesnila N, Shenton ME, Lin AP, Koerte IK (2021) Translational neuroimaging in mild traumatic brain injury. J Neurosci Res doi: 10.1002/jnr.24840.

Wittenberg GF, Schaechter JD (2009) The neural basis of constraint-induced movement therapy. Curr Opin Neurol 22:582-588.

Wolf SL, Winstein CJ, Miller JP, Taub E, Uswatte G, Morris D, Giuliani C, Light KE, Nichols-Larsen D, Investigators E (2006) Effect of constraint-induced movement therapy on upper extremity function 3 to 9 months after stroke: the EXCITE randomized clinical trial. JAMA 296:2095-2104.

Wolf SL, Winstein CJ, Miller JP, Thompson PA, Taub E, Uswatte G, Morris D, Blanton S, Nichols-Larsen D, Clark PC (2008) Retention of upper limb function in stroke survivors who have received constraint-induced movement therapy: the EXCITE randomised trial. Lancet Neurol 7:33-40.

Zhang ZG, Buller B, Chopp M (2019) Exosomes- beyond stem cells for restorative therapy in stroke and neurological injury. Nat Rev Neurol 15:193-203.

Zhao S, Zhao M, Xiao T, Jolkkonen J, Zhao C (2013) Constraint-induced movement therapy overcomes the intrinsic axonal growth-inhibitory signals in stroke rats. Stroke 44:1698-1705.

Zheng T, Yuan Y, Yang H, Du J, Wu S, Jin Y, Wang Z, Liu D, Shi Q, Wang X, Liu L (2020) Evaluating the therapeutic effect of low-intensity transcranial ultrasound on traumatic brain injury with diffusion kurtosis imaging. J Magn Reson Imaging 52:520-531.

P-reviewers: Zhang J, Petrus E; C-Editor: Zhao M; S-Editor: Li CH; L-Editors: McCollum L, Li CH, Song LP; T-Editor: Jia Y